YC-1: A Potential Anticancer Drug Targeting Hypoxia-Inducible Factor 1

Eun-Jin Yeo, Yang-Sook Chun, Young-Suk Cho, Jinho Kim, June-Chul Lee, Myung-Suk Kim, Jong-Wan Park

Background: **Hypoxia-inducible factor 1 alpha (HIF-1α), a component of HIF-1, is expressed in human tumors and renders cells able to survive and grow under hypoxic (low-oxygen) conditions. YC-1, 3-(5′-hydroxymethyl-2′-furyl)-1-benzylindazole, an agent developed for circulatory disorders that inhibits platelet aggregation and vascular contraction, inhibits HIF-1 activity *in vitro*. We tested whether YC-1 inhibits HIF-1 and tumor growth *in vivo*. *Methods:* Hep3B hepatoma, NCI-H87 stomach carcinoma, Caki-1 renal carcinoma, SiHa cervical carcinoma, and SK-N-MC neuroblastoma cells were grown as xenografts in immunodeficient mice (69 mice total). After the tumors were 100–150 mm^3, mice received daily intraperitoneal injections of vehicle or YC-1 (30 μg/g) for 2 weeks. HIF-1α protein levels and vascularity in tumors were assessed by immunohistochemistry, and the expression of HIF-1-inducible genes (vascular endothelial growth factor, aldolase, and enolase) was assessed by reverse transcription–polymerase chain reaction. All statistical tests were two-sided. *Results:* Compared with tumors from vehicle-treated mice, tumors from YC-1-treated mice were statistically significantly smaller ($P<.01$ for all comparisons), expressed lower levels of HIF-1α ($P<.01$ for all comparisons), were less vascularized ($P<.01$ for all comparisons), and expressed lower levels of HIF-1-inducible genes, regardless of tumor type. *Conclusions:* The inhibition of HIF-1α activity in tumors from YC-1-treated mice is associated with blocked angiogenesis and an inhibition of tumor growth. YC-1 has the potential to become the first antiangiogenic anticancer agent to target HIF-1α. [J Natl Cancer Inst 2003; 95:516–25]**

Hypoxia, a reduction in tissue oxygen levels below physiologic levels, commonly develops within solid tumors because tumor cell proliferation is greater than the rate of blood vessel formation. Thus, the increase in tumor mass results in aberrant vasculature formation, which compromises the blood supply *(1).* However, tumor hypoxia also stimulates the increased expression of vascular endothelial growth factor (VEGF), which promotes angiogenesis, which is in turn essential for meeting the metabolic requirements of tumor growth *(2).* Hypoxia also contributes to tumor progression to a more malignant phenotype because cells surviving under hypoxic conditions often become resistant to radiotherapy and chemotherapy *(3).* Thus, factors that regulate hypoxic events may be good targets for anticancer therapy.

One such target is hypoxia-inducible factor 1 (HIF-1). HIF-1 is a key transcription factor that regulates the blood supply through its effects on the expression of VEGF *(4).* The biologic activity of HIF-1, a heterodimer composed of HIF-1α and HIF-1β subunits *(5),* depends on the amount of HIF-1α, which is tightly regulated by oxygen tension. Under normoxic conditions, the HIF-1α protein is unstable. The instability is regulated, in part, by the binding to the von Hippel–Lindau tumor suppressor protein *(6).* This binding occurs after the hydroxylation of the two HIF-1α proline residues by HIF-prolyl hydroxylases *(7–9).* The von Hippel–Lindau protein is one of the components of the multiprotein ubiquitin–E3–ligase complex, which mediates the ubiquitylation of HIF-1α, targeting it for proteasomal proteolysis *(10).* Under hypoxic conditions, however, proline hydroxylation is inhibited, eliminating binding between HIF-1α and the von Hippel–Lindau protein, and allowing HIF-1α to become stable.

A growing body of evidence indicates that HIF-1 contributes to tumor progression and metastasis. In human tumors, HIF-1α is overexpressed as a result of intratumoral hypoxia and genetic alterations affecting key oncogenes (HER2, FRAP, H-RAS, and c-SRC) and tumor suppressor genes (von Hippel–Lindau, PTEN, and p53) *(11).* Immunohistochemical analyses show that HIF-1α is present at higher levels in human tumors than in normal tissues *(12).* Moreover, the expression of HIF-1α in various solid tumors has been associated with tumor aggressiveness, vascularity, treatment failure, and mortality *(13).* In addition, tumor growth and angiogenesis in xenograft tumors also depends on HIF-1 activity and on the expression level of HIF-1α *(14).*

While searching for an antiangiogenic agent that would inhibit HIF-1 activity, we identified a novel pharmacologic action of YC-1. YC-1, 3-(5′-hydroxymethyl-2′-furyl)-1-benzylindazole, inhibits platelet aggregation and vascular contraction by activating soluble guanylyl cyclase and was originally developed as a potential therapeutic agent for circulation disorders *(15,16).* However, we found that YC-1 inhibits HIF-1 activity *in vitro (17).* YC-1 completely blocks HIF-1α expression at the post-transcriptional level and consequently inhibits the transcription factor activity of HIF-1 in hepatoma cells cultured under hypoxic conditions, suggesting that these effects of YC-1 are likely to be linked with the oxygen-sensing pathway and not

Affiliation of authors: E.-J. Yeo, Y.-S. Cho, J. Kim, M.-S. Kim, J.-W. Park (Department of Pharmacology, BK21 Human Life Sciences), Y.-S. Chun, J.-C. Lee (Human Genome Research Institute, Cancer Research Institute), Seoul National University College of Medicine, Seoul, Korea.

Correspondence to: Jong-Wan Park, M.D., Ph.D., Department of Pharmacology, Seoul National University College of Medicine, 28 Yongon-dong, Chongno-gu, Seoul 110–799, Korea (e-mail: parkjw@plaza.snu.ac.kr).

See "Notes" following "References."

Journal of the National Cancer Institute, Vol. 95, No. 7,

with the activation of soluble guanylyl cyclase. In this study, we tested whether YC-1 targets HIF-1 and tumor angiogenesis *in vivo.*

Materials and Methods

Materials

YC-1 was purchased from AG Scientific Inc. (San Diego, CA), resuspended in dimethyl sulfoxide (DMSO) at a stock concentration of 120 mg/mL, and stored at –30 °C. All culture media and fetal bovine serum (FBS) were purchased from Life Technologies, Grand Island, NY.

Cell Culture

The Hep3B hepatoma, Caki-1 renal carcinoma, SiHa cervical carcinoma, and SK-N-MC neuroblastoma cell lines were obtained from the American Type Culture Collection (ATCC; Manassas, VA). The NCI-H87 stomach carcinoma cell line was obtained from the Korean Cell Line Bank (Seoul, Korea). Hep3B cells were cultured in α-modified Eagle medium; Caki-1, SiHa, and SK-N-MC cells, in Dulbecco's modified Eagle medium; and NCI-H87 cells, in RPMI-1640 medium. All culture media were supplemented with 10% heat-inactivated FBS, penicillin (100 U/mL), and streptomycin (100 μg/mL). All cells were grown in a humidified atmosphere containing 5% CO_2 at 37 °C, in which the oxygen tension in the incubator (model 9108MS2; Vision Sci Co., Seoul, Korea) was held at either 140 mmHg (20% O_2, v/v; normoxic conditions) or 7 mmHg (1% O_2, v/v; hypoxic conditions). The natural killer (NK)-sensitive YAC-1 mouse lymphoma cell line was obtained from the ATCC and maintained in RPMI-1640 medium supplemented with 10% FBS, 1% L-glutamine, 1% nonessential amino acids, 1% sodium pyruvate, penicillin (100 U/mL), and streptomycin (100 μg/mL).

Xenografts of Human Tumors

Male nude (BALB/cAnNCrj–nu/nu) mice were purchased from Charles River Japan Inc. (Shin-Yokohama, Japan). The animals were housed in a pathogen-free room under controlled temperature and humidity. All animal procedures were performed according to the established procedures of the Seoul National University Laboratory Animal Maintenance Manual.

Eighty mice aged 7–8 weeks were injected with tumor cells for the xenograft experiments. Sixty-nine mice bearing tumors were used for the experiments; the other 11 mice were excluded because of technical problems associated with the injection or because of lack of tumor growth. Viable Hep3B cells (5×10^6) were injected subcutaneously into the flanks of 25 of the 69 mice. The mice were immediately randomly assigned to one of three groups. The first group (n = 12) was a control group and received the vehicle (DMSO). The second group (n = 7) received daily intraperitoneal injections of YC-1 (30 μg/g) beginning the day after the injection of Hep3B cells and continuing for 2 weeks. The third group (n = 6) received daily intraperitoneal injections of YC-1 (30 μg/g) for 2 weeks after the Hep3B tumors measured 100–150 mm^3, after approximately 40 days.

NCI-H87, SiHa, SK-N-MC, or Caki-1 tumor cells (5×10^6) were injected subcutaneously into the flanks of the other 44 mice. Of the mice in each group, 13, 10, 10, and 11, respectively, developed tumors. The tumor-bearing mice in each group were randomly assigned to either a control group or an experimental group. After the tumors reached an approximate volume of 100–150 mm^3, the mice in the experimental group received daily intraperitoneal injections of YC-1 (30 μg/g) for 2 weeks. The mice in the control groups received daily intraperitoneal injections of DMSO.

For all mice, tumors were measured in two dimensions with calipers every 2 or 3 days, and the tumor volumes were calculated using the following formula: volume $= a \times b^2/2$, where a is the width at the widest point of the tumor and b is the width perpendicular to a. The results from individual mice were plotted as average tumor volume versus time.

Semiquantitative Reverse Transcription–Polymerase Chain Reaction

To quantify mRNAs for HIF-1α, HIF-1-regulated genes (VEGF, enolase 1, aldolase A), and β-actin (used as a control), we performed a highly sensitive, semiquantitative reverse transcription–polymerase chain reaction (RT–PCR), as described previously *(18).* Total RNAs were isolated from cultured cells or grafted tumors using TRIzol (Life Technologies). After we verified the RNA quality on a 1% denaturing agarose gel, 1 μg of total RNA was added to a 50-μL RT–PCR reaction mixture, containing 5 μCi [α-^{32}P]dCTP (NEN, Boston, MA) and 250 n*M* of each primer pair. The RT–PCR was performed using one cycle of reverse transcription at 48 °C for 1 hour and then 18 PCR cycles, in which one cycle consisted of a denaturation step at 94 °C for 30 seconds, an annealing step at 53 °C for 30 seconds, and an elongation step at 68 °C for 1 minute. The resulting PCR fragments (5 μL) were electrophoresed through a 4% polyacrylamide gel at 120 V in a 0.3× Tris–borate–EDTA (TBE) buffer at 4 °C. The gels were dried and then autoradiographed. The intensity of each PCR product was determined with a Sony XC-77 CCD camera and a Microcomputer Imaging Device model 4 (MCID-M4) image analysis system (Imaging Research Inc., St. Catharines, Ontario, Canada).

The nucleotide sequences of the primer pairs (5′ to 3′) were AACTTTCTGCTGTCTTGG and TTTGGTCTGCATTCACAT for VEGF, GTCATCCTCTTCCATGAGAC and AGGTAGAT GTGGTGGTCACT for aldolase A, AAGAAACTGAACGTCA CAGA and GATCTTCGATAGACACCACT for enolase 1, CCCCAGATTCAGGATCAGACA and CCATCATGTTCCAT TTTTCGC for HIF-1α, and AAGAGAGGCATCCTCACCCT and ATCTCTTGCTCGAAGTCCAG for β-actin.

Immunoblotting and Immunoprecipitation

Immunoblotting was used to detect HIF-1α protein in cultured cells, as described *(17).* Cells were centrifuged at 1000*g* for 5 minutes at 4 °C and washed twice with ice-cold phosphate-buffered saline (PBS). Cells were then resuspended in 10 packed-cell volumes of a lysis buffer consisting of 10 m*M* Tris [pH 7.4], 130 m*M* NaCl, 2 m*M* EDTA, 1% Nonidet P-40, 0.5 m*M* dithiothreitol, and 0.5 m*M* phenylmethylsulfonyl fluoride. Proteins (20 μg) in the cell extract were separated on 6.5% sodium dodecyl sulfate (SDS) polyacrylamide gels and then transferred to Immobilon-P membranes (Millipore, Bedford, MA). Membranes were blocked with 5% nonfat milk in Tris-buffered saline (TBS) containing 0.1% Tween-20 (TTBS) at room temperature for 1 hour and then incubated overnight at 4 °C with rabbit anti-HIF-1α *(18)* diluted 1 : 1000 in 5% nonfat milk in TTBS. Horseradish peroxidase-conjugated anti-rabbit antiserum (Zymed Laboratories, Inc., South San Francisco, CA) was used as a secondary antibody (1 : 5000 dilution in 5% nonfat

milk in TTBS, 2-hour incubation), and the antigen–antibody complexes were visualized by using an Enhanced Chemiluminescence Plus kit (Amersham Biosciences, Piscataway, NJ). Protein loading was controlled by probing the membranes for β-actin protein.

VEGF, platelet-derived growth factor (PDGF)-A, PDGF-B, and β-actin proteins in tumor tissue were detected using a mouse monoclonal anti-VEGF antibody (Santa Cruz Biotechnology, Inc., Santa Cruz, CA) at a dilution of 1 : 1000, a mouse monoclonal anti-PDGF-A antibody (Santa Cruz Biotechnology) at a dilution of 1 : 5000, a rabbit polyclonal anti-PDGF-B antibody (Santa Cruz Biotechnology) at a dilution of 1 : 1000, a mouse monoclonal anti-β-actin antibody (Santa Cruz Biotechnology) at a dilution of 1 : 5000 followed by incubation with a horseradish peroxidase-conjugated anti-mouse or anti-rabbit antiserum (Zymed Laboratories).

For the immunoprecipitation of HIF-1α in tumor tissues, tissue lysates in the lysis buffer (150 μg of protein) were incubated with 10 μL of the rabbit anti-HIF-1α antiserum overnight at 4 °C and then incubated with protein A-Sepharose beads (Amersham Biosciences) at a dilution of 1 : 100 for 2 hours. After the antigen–antibody–protein A complexes were washed extensively with the lysis buffer, the immunocomplexes were eluted by boiling for 3 minutes in a sample buffer containing 2% SDS and 10 m*M* dithiothreitol, subjected to SDS-PAGE (SDS–polyacrylamide gel electrophoresis), and then immunoblotted using a rat anti-HIF-1α antibody *(19)*.

Conditioned Media and VEGF Enzyme-Linked Immunosorbent Assay

Hep3B cells were plated in a six-well plate at a density of 1×10^5 cells/well in α-modified Eagle medium supplemented with 10% heat-inactivated FBS and incubated overnight. Cells were treated with YC-1 (0.01–10 μ*M*) or vehicle (DMSO) for 5 minutes and were then subjected to normoxia or hypoxia for 24 hours. VEGF levels in the conditioned media were quantified by using the Quantikine human VEGF Immunoassay kit (R&D Systems, Minneapolis, MN) according to the manufacturer's recommended protocol. The VEGF concentrations were quantified by comparison with a series of VEGF standard samples included in the assay kit.

Tumor Histology and Immunohistochemistry for HIF-1α, CD31, and Asialo GM1

The day after the last injection of YC-1 or vehicle, the mice were killed, and the tumors were removed. The tumors were fixed with formalin and embedded in paraffin. Serial sections (6-μm thick) were cut from each paraffin block. One section was stained with hematoxylin–eosin (H&E) for histologic assessment. Other sections were immunochemically stained for HIF-1α, for the endothelial cell marker CD31, or for the NK cell marker asialo GM1. The sections were deparaffinized, rehydrated through a graded alcohol series, and heated in 10 m*M* sodium citrate (pH 6.0) for 5 minutes in a microwave to retrieve the antigens. Nonspecific sites were blocked with a solution containing 2.5% bovine serum albumin (Sigma-Aldrich Corp., St. Louis, MO) and 2% normal goat serum (Life Technologies) in PBS (pH 7.4) for 1 hour, and the sections were then incubated overnight at 4 °C with rabbit polyclonal anti-CD31 antibody (1 : 100 dilution in the blocking solution; Santa Cruz Biotechnology), rabbit polyclonal anti-asialo GM1 antibody (Wako Chemicals, Chuo-Ku, Osaka, Japan; 1 : 100 dilution in the blocking solution), or rat anti-HIF-1α antibody (1 : 100 dilution in the blocking solution), as described previously *(20)*. Negative control sections were incubated with the diluent (blocking solution) in the absence of any primary antibodies. The sections were then washed and incubated with appropriate biotinylated secondary antibodies, and the avidin–biotin–horseradish peroxidase complex was used to localize the bound antibodies, with diaminobenzidine as the final chromogen. All immunostained sections were lightly counterstained with hematoxylin.

For histologic assessment, HIF-1α-positive cells, CD31-positive microvessels, and necrosis were identified at magnifications of ×200, ×100, and ×40, respectively, and examined using a Sony XC-77 CCD camera and a Microcomputer Imaging Device model 4 (MCID-M4) image analysis system. The expression of HIF-1α and vessel density was measured by counting the numbers of immunopositive cells and vessel profiles (identified by CD31 staining) per square millimeter in each image. The extent of necrosis was measured by calculating the necrotic area per 6.25 mm^2. We analyzed 10 or more different sections per xenograft tumor.

NK Cell Activity

Splenic lymphocytes from 12 nude mice were used to determine the effect of YC-1 on NK cell activity *in vitro* and *in vivo*. Individual spleens were homogenized in PBS by passing tissues through steel mesh using a plunger and centrifuged over a Ficoll-Paque (Amersham Biosciences) gradient at 400*g* at room temperature for 30 minutes to isolate the lymphocyte population. The lymphocytes were removed and washed three times in PBS. NK cell activity in the total lymphocyte population was assessed using a 4-hour ^{51}Cr-release assay with NK-sensitive YAC-1 cells as the target cell population. The YAC-1 cells were labeled with sodium chromate ($Na_2{}^{51}CrO_4$) at 0.25 mCi/mL for 1.5 hours at 37 °C in a humidified atmosphere containing 5% CO_2, as described *(21)*.

To examine the *in vitro* effect of YC-1 on NK cell activity, splenic lymphocytes (6.25×10^4 to 5×10^5) were incubated with YC-1 (0.1–10 μ*M*) or DMSO for 24 hours and then incubated at the indicated effector : target cell ratio with 1×10^4 ^{51}Cr-labeled YAC-1 cells in 96-well round-bottom plates at 37 °C in a humidified atmosphere containing 5% CO_2. After 4 hours, the plates were centrifuged at 200*g* at 4 °C for 10 minutes, and 100-μL samples of medium were removed and counted for 1 minute in a gamma counter. Splenic lymphocytes taken from a single mouse were used in each experiment. Each assay was repeated three times, and the average value is the result from one experiment. Results are expressed as the mean of the average values from four separate experiments and 95% confidence intervals (CIs).

To examine the *in vivo* effect of YC-1 on NK cell activity, mice received a daily intraperitoneal injection of DMSO ($n = 4$) or of YC-1 (30 μg/g; $n = 4$) for 2 weeks. Splenic lymphocytes were isolated from each mouse and tested immediately for NK cell activity. The spontaneous release of ^{51}Cr from YAC-1 cells was usually lower than 10% of the total ^{51}Cr loaded. NK cell activity was calculated as follows: (experimental release minus spontaneous release)/(total release minus spontaneous release) × 100. Each assay was repeated three times, and the average value is the result from one experiment. Results are expressed as the mean of four separate experiments and 95% CIs.

Statistical Analysis

All data were analyzed using Microsoft Excel 2000 software (Microsoft Corp., Redmond, WA). The Mann–Whitney *U* test (SPSS, version 10.0; Statistical Package for Social Sciences, Chicago, IL) was used to compare VEGF levels in culture media, the number of HIF-1α-positive cells, the number of vessels, NK cell activities, and tumor volumes (NCI-H87, SiHa, SK-N-MC, Caki-1) between the control and the YC-1 treated groups. Tumor volumes in the control and two YC-1-treated Hep3B groups were compared using an analysis of variance (ANOVA) followed by Duncan's multiple range test. Differences were considered statistically significant when $P<.05$. All statistical tests were two-sided.

Results

Effect of YC-1 on the HIF-1-Mediated Expressions of Hypoxia-Inducible Genes

Previously, we found that YC-1 treatment inhibits HIF-1α protein expression and decreases the mRNA levels of erythropoietin and VEGF in Hep3B cells cultured under hypoxic conditions. To investigate the inhibitory effect of YC-1 on HIF-1-mediated hypoxic responses, Hep3B cells were treated with YC-1 under hypoxic conditions. The HIF-1α protein level increased in cells cultured under these conditions for 4 hours without YC-1 but underwent a dose-dependent decrease in cells cultured with YC-1 (Fig. 1, A). The expression of several HIF-1-regulated genes (VEGF, aldolase A, and enolase 1) showed a dose-dependent decrease in cells cultured with YC-1 for 16 hours, whereas the expression of β-actin mRNA was not affected (Fig. 1, B). The HIF-1α mRNA level was also relatively unchanged in cells cultured with YC-1, suggesting that YC-1-mediated decrease in HIF-1α protein expression occurs at a post-transcriptional level.

To assess whether the decreased VEGF mRNA levels affected levels of VEGF protein secreted into the medium, we measured VEGF protein levels in Hep3B cell-conditioned medium. After 24 hours, the VEGF protein level in medium from cells cultured under hypoxic conditions (mean = 1208 pg/mL, 95% CI = 1112 to 1304 pg/mL; $P<.001$ versus normoxic conditions) was more than twice that from cells cultured under normoxic conditions (mean = 559 pg/mL, 95% CI = 392 to 726 pg/mL) (Fig. 1, C). Compared with the VEGF protein level in medium from untreated cells grown under hypoxic conditions, the VEGF protein level in medium from cells cul-

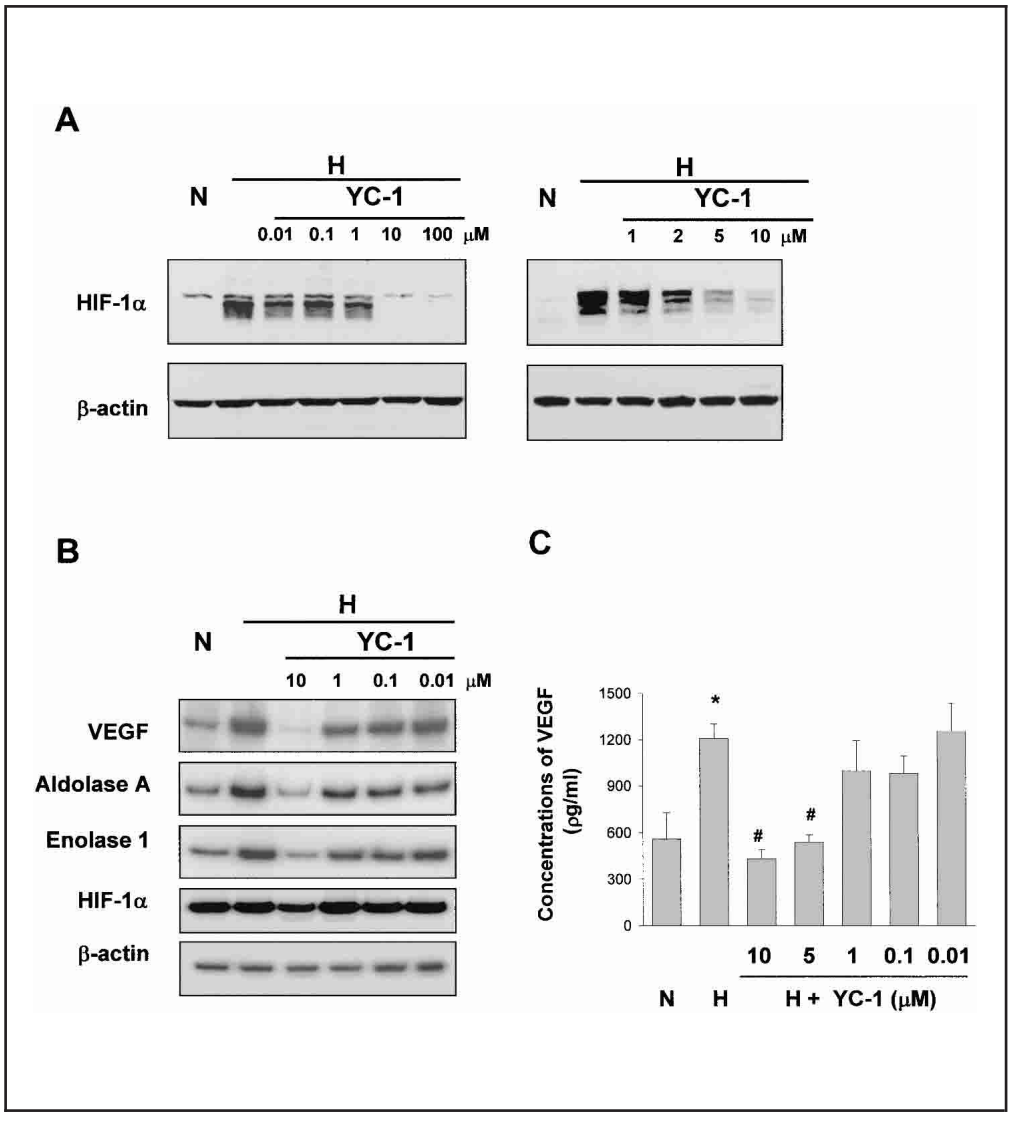

Fig. 1. The effects of YC-1 on the expression of hypoxia-inducible factor 1 alpha (HIF-1α) and hypoxia-inducible genes in Hep3B hepatoma cells. **A**) Hep3B cells were treated with the indicated concentrations of YC-1 5 minutes before being cultured for 4 hours under normoxic (N, 20% O_2 v/v) or hypoxic (H, 1% O_2 v/v) conditions. Expression of HIF-1α and β-actin proteins was analyzed by immunoblotting with a rabbit anti-HIF-1α antibody and a rabbit anti-β-actin antibody, respectively. Proteins were visualized by enhanced chemiluminescence. **B**) mRNAs for vascular endothelial growth factor (VEGF), aldolase A, enolase 1, HIF-1α, and β-actin were isolated from Hep3B cells that had been treated with the indicated concentrations of YC-1 and cultured under normoxic or hypoxic conditions for 16 hours. mRNA expression was analyzed by semiquantitative reverse transcription–polymerase chain reaction. **C**) The amount of VEGF protein in conditioned medium from Hep3B cells that had been treated with the indicated concentrations of YC-1 and cultured under normoxic or hypoxic conditions for 24 hours was measured using an enzyme-linked immunosorbent assay (ELISA) kit. The VEGF concentrations were quantified by comparison with a series of VEGF standard samples included in the assay kit. VEGF level in each experiment was measured twice. **Bars** represent the mean of four separate experiments with the upper 95% confidence interval. * denotes a statistically significant difference relative to control supernatants from cells cultured under normoxic conditions ($P<.001$); # denotes a statistically significant difference relative to control supernatants from cells cultured under hypoxic conditions ($P<.001$).

tured with YC-1 was reduced in a dose-dependent manner ($P<.001$) (Fig. 1, C).

We next examined whether the effects of YC-1 were specific to Hep3B cells by assessing the expression of HIF-1α protein and VEGF mRNA in other tumor cell lines (NCI-H87, SiHa, SK-N-MC, and Caki-1) cultured under hypoxic conditions in the absence or presence of YC-1. HIF-1α protein and VEGF mRNA were induced in all cell lines cultured under hypoxic conditions in the absence of YC-1 (Fig. 2). The levels of HIF-1α protein and VEGF mRNA were dose-dependently reduced in cells cultured under hypoxic conditions in the presence of YC-1 (Fig. 2). These results confirm that YC-1 inhibits the HIF-1-mediated induction of hypoxia-inducible genes, regardless of the tumor cell type.

Effects of YC-1 on Tumor Growth *In Vivo*

Because of the observed *in vitro* effects of YC-1, we investigated whether YC-1 inhibits angiogenesis in solid tumors by suppressing the activity of HIF-1 and whether YC-1 inhibits tumor growth *in vivo*. Mice injected with human tumor cells were treated daily with YC-1 for 2 weeks. Tumors in YC-1-treated mice were visibly smaller than those in vehicle-treated mice (Fig. 3, A). The change in tumor size was measured and plotted as average tumor size versus time (Fig. 3, B). Tumor growth was minimal in mice treated with YC-1 the day after the tumor cells were injected (the last day of the experiment: mean = 422 mm^3, 95% CI = 283 to 561 mm^3; $P<.001$ versus vehicle-treated group, mean = 1082 mm^3, 95% CI = 880 to 1284 mm^3) and was halted in mice treated with YC-1 after the tumors had become established (mean = 126 mm^3, 95% CI = 97 to 155 mm^3; $P<.001$ versus vehicle-treated group). NCI-H87 (Fig. 3, C), SiHa (Fig. 3, D), SK-N-MC (Fig. 3, E), and Caki-1 (Fig. 3, F) xenograft tumors were also statistically significantly smaller in mice treated with YC-1 than in mice treated with the vehicle ($P<.01$ for all comparisons). These results indicate that YC-1 effectively inhibits tumor growth in tumor-bearing mice.

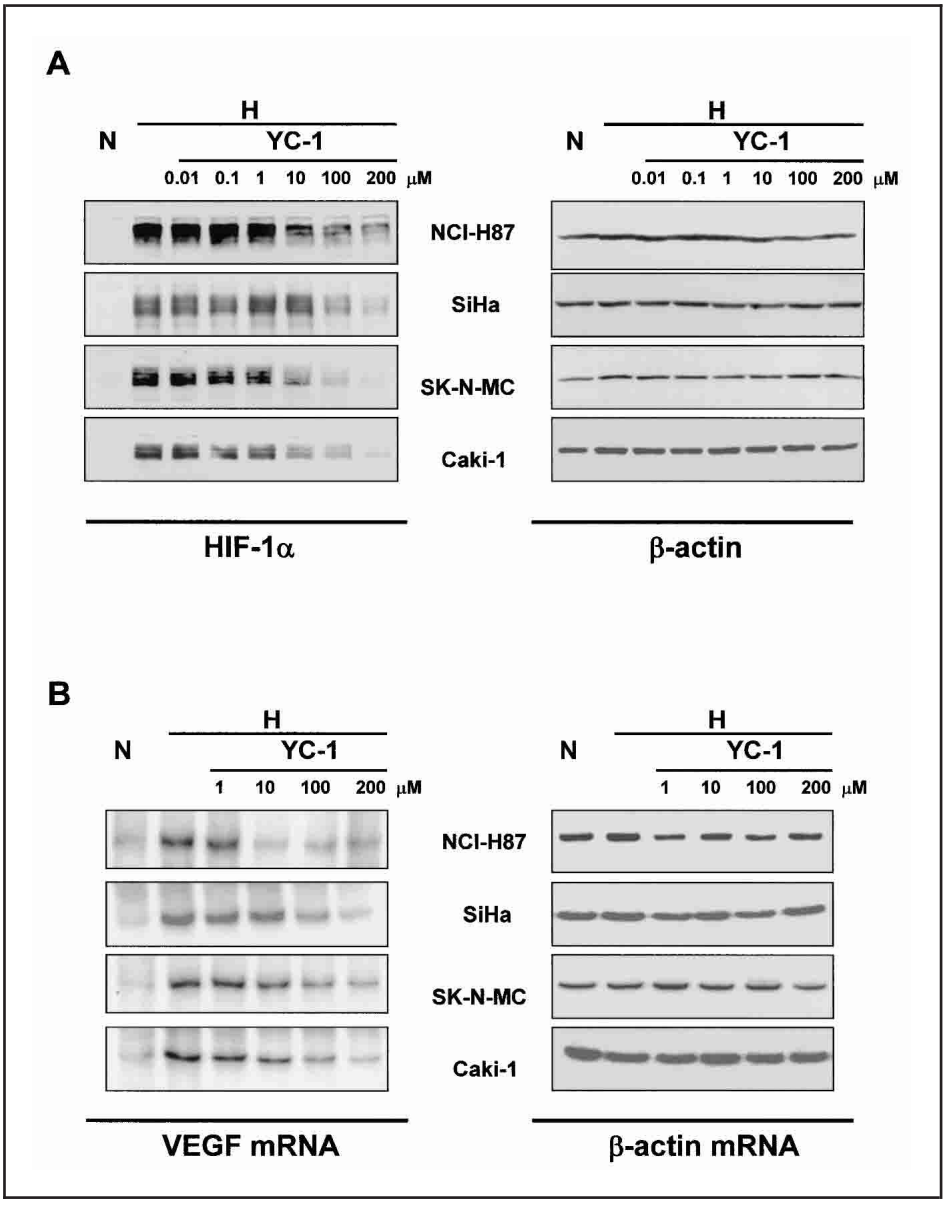

Fig. 2. The effect of YC-1 on the expression of hypoxia-inducible factor 1 alpha (HIF-1α) and the hypoxia-inducible gene vascular endothelial growth factor (VEGF) in cancer cells of different origin. **A**) NCI-H87 gastric carcinoma, SiHa cervical carcinoma, SK-N-MC neuroblastoma, and Caki-1 renal carcinoma cells were treated with the indicated concentrations of YC-1 5 minutes before being cultured under normoxic (N, 20% O_2 v/v) or hypoxic (H, 1% O_2 v/v) conditions for 4 hours. Levels of HIF-1α and β-actin proteins were analyzed by immunoblot analysis using a rabbit anti-HIF-1α antibody or a rabbit anti-β-actin antibody. Proteins were visualized by enhanced chemiluminescence. **B**) mRNAs for VEGF and β-actin were isolated from cells that had been treated with the indicated concentrations of YC-1 and cultured under normoxic or hypoxic conditions for 16 hours. mRNA expression was analyzed by semiquantitative reverse transcription–polymerase chain reaction.

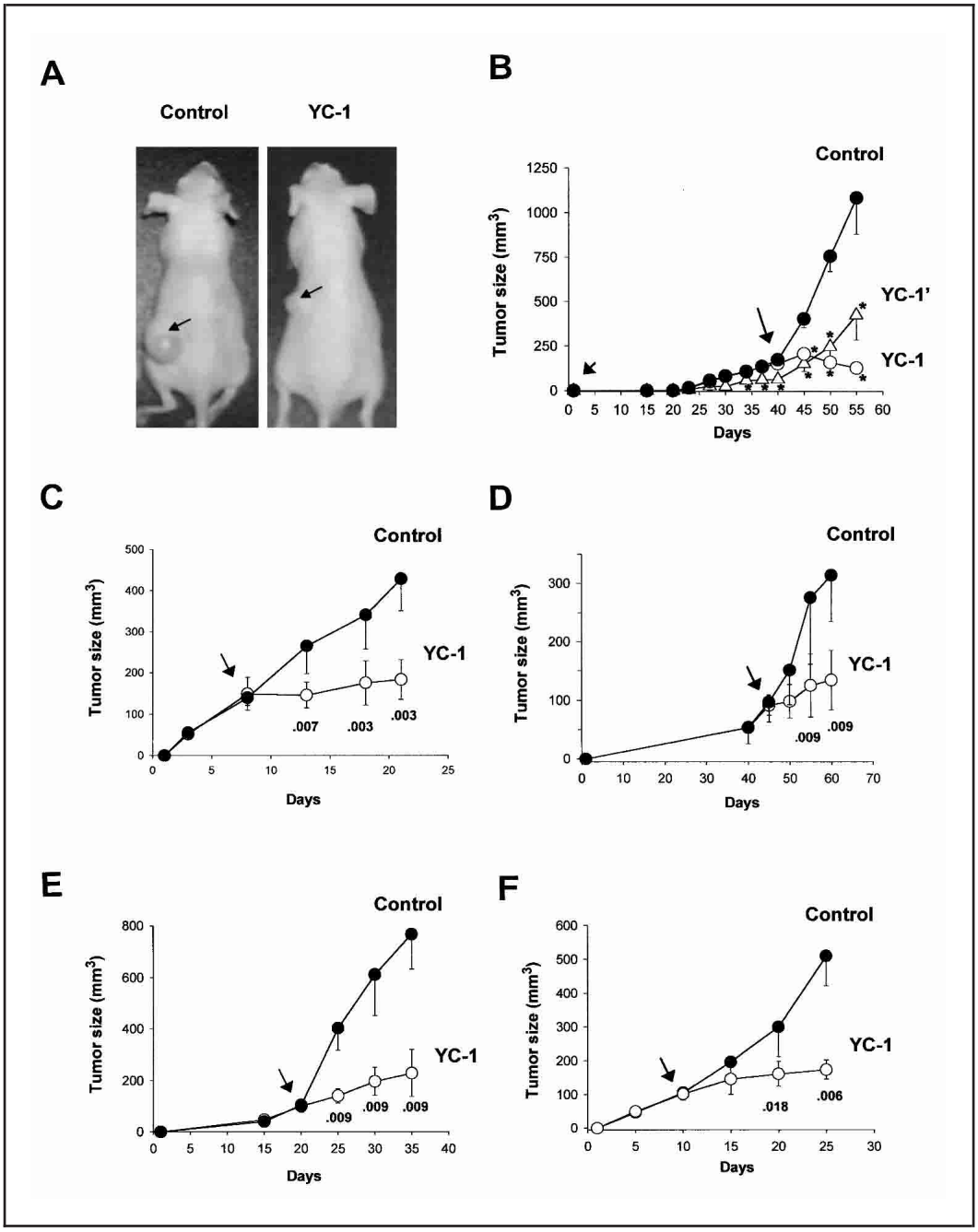

Fig. 3. The effect of YC-1 on the development of xenografted human tumors. Viable Hep3B hepatoma (**A** and **B**), NCI-H87 gastric carcinoma (**C**), SiHa cervical carcinoma (**D**), SK-N-MC neuroblastoma (**E**), or Caki-1 renal carcinoma (**F**) cells (5×10^6) were injected subcutaneously into the flanks of male nude mice. After the tumors reached 100–150 mm^3 in size (indicated by **long arrow** in **B** and **short arrows** in **C–F**), mice received an intraperitoneal injection of YC-1 (30 μg/g) or vehicle (dimethyl sulfoxide [DMSO]) daily for 2 weeks. Tumor size was measured over time. **A**) Hep3B xenografts on the flanks of mice treated with vehicle only (Control) or with YC-1 for 2 weeks. The **arrows** indicate Hep3B tumors on mouse flanks. **B**) Beginning 2 days after the injection of the Hep3B cells, some mice received injections of YC-1 daily for 2 weeks (indicated by a **short arrow**). **Solid circles** = vehicle, **open circles** = YC-1 (treatment of established tumors), and **open triangles** = YC-1′ (treatment before established tumors). Each data point represents the mean (n = 12 for control; n = 6 for YC-1; n = 7 for YC-1′), and **error bars** show 95% confidence intervals. Statistical significance of differences in tumor sizes between the vehicle- and YC-1-treated groups for mice with Hep3B tumors (**B**) were compared using analysis of variance (ANOVA) and Duncan's multiple range tests. * denotes $P<.001$ relative to the control. Differences between tumor sizes in the vehicle- and YC-1-treated groups for mice with other tumors (**C–F**) were compared using a Mann–Whitney *U* test. **Numbers beneath the error bars** represent the *P* value of the difference relative to the control.

Effects of YC-1 on Angiogenesis, HIF-1α Protein, and VEGF Expression

To determine the mechanism by which YC-1 inhibits tumor growth, we examined Hep3B tumors morphologically and biochemically. H&E-stained tumor sections from vehicle-treated mice revealed well-developed blood vessels containing red blood cells and several mitotic figures (Fig. 4, A). By contrast, tumor sections from YC-1-treated mice revealed frequent acinus formation without well-developed blood vessels (Fig. 4, A).

To determine whether the inhibitory effect of YC-1 on tumor growth is associated with the suppression of tumor angiogenesis, we examined the distribution of the endothelial marker CD31. Few CD31-immunopositive vessels were observed in tumor sections from YC-1-treated mice, whereas many vessels were observed in tumor sections from vehicle-treated mice (Fig. 4, B).

Because HIF-1 is important in angiogenesis, we next assessed HIF-1α expression in tumor sections from vehicle- and YC-1-treated mice (Fig. 4, C). Hep3B tumors from vehicle-treated mice showed HIF-1α protein in both the nucleus and perinuclear areas but only in relatively hypoxic regions away from blood vessels (Fig. 4, C). By contrast, tumor sections from YC-1-treated mice showed no HIF-1α-immunoreactive cells (Fig. 4, C).

We quantified the numbers of HIF-1α-positive cells and CD31-positive vessels in tumor sections from vehicle- and YC-1-treated mice (Fig. 5). Regardless of tumor cell origin, the expression of HIF-1α protein and blood vessel formation was statistically significantly lower in mice treated with YC-1 for 2 weeks than in vehicle-treated mice ($P<.01$ for all comparisons) (Fig. 5).

We also measured the extent of necrosis in Hep3B tumor sections stained with H&E. No statistically significant difference

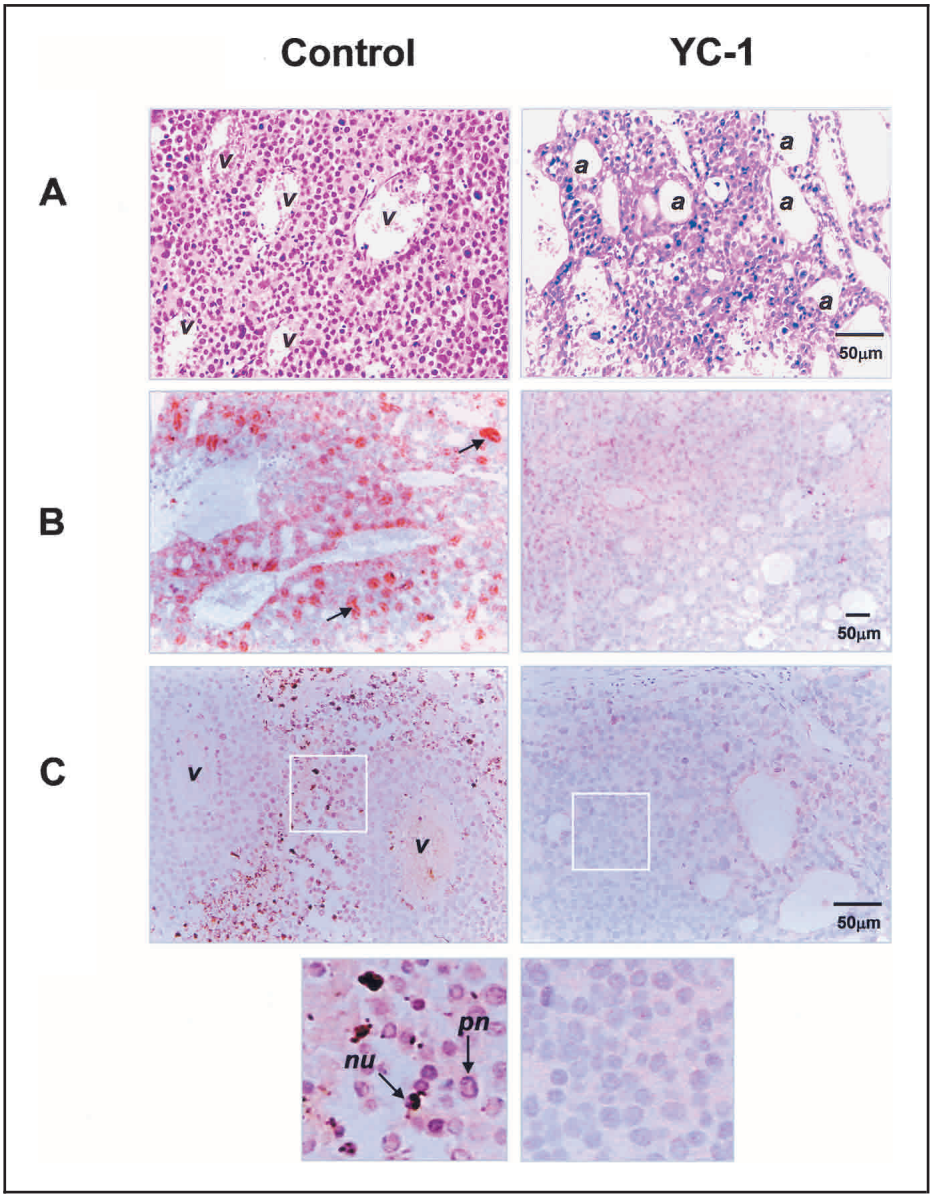

Fig. 4. Histopathology and immunohistochemistry for Hep3B hepatoma tumors grown in nude mice. Viable Hep3B cells (5×10^6) were injected subcutaneously into the flanks of male nude mice. After the tumors reached 100–150 mm^3 in size, mice received an intraperitoneal injection of YC-1 (30 μg/g) or vehicle (dimethyl sulfoxide [DMSO]) daily for 2 weeks. After the last treatment, the mice were euthanized and the tumors were removed, fixed with formalin, and embedded in paraffin. Tumor sections were cut from the paraffin blocks and stained with hematoxylin and eosin (**A**) or processed for immunohistochemical staining with an anti-CD31 antibody to detect endothelial cells (**B**) or with a rat anti-HIF-1α antibody for hypoxia-inducible factor 1 alpha (HIF-1α) (**C**). All immunostained sections were developed using the avidin–biotin–horseradish peroxidase method with diaminobenzidine as the chromagen. All sections were lightly counterstained with hematoxylin. **Arrows** indicate CD31-positive vessels in B and HIF-1α-positive cells in C. **v** = vessel; **a** = acinus; **nu** = nuclear staining; **pn** = perinuclear staining.

in the percentage of necrosis was found between tumors from vehicle-treated mice (40 lesions examined; mean = 16.3%, 95% CI = 12.2% to 20.4%) and those from YC-1-treated mice (six lesions examined; mean = 18.3%, 95% CI = 10.2% to 26.4%; $P = .17$). Similarly, for the other tumor types, the differences in the extent of necrosis between tumors from vehicle- and YC-1-treated mice were not statistically significant (data not shown).

To confirm the effects of YC-1 on HIF-1α expression in Hep3B tumors, we isolated the HIF-1α protein by immunoprecipitation and immunoblotting. HIF-1α was detected by immunoprecipitation in tumor lysates incubated with anti-HIF-1α antibody, but not in those incubated with a preimmune serum (data not shown). The level of HIF-1α protein expression was markedly lower in YC-1-treated tumors than in vehicle-treated tumors (Fig. 6, A). In addition, levels of VEGF protein and mRNA, and of aldolase and enolase mRNAs were also lower in YC-1-treated tumors than in vehicle-treated tumors (Fig. 6, A and B). The decreased expression of VEGF, aldolase, and enolase may in turn account for the blocked angiogenesis and the growth retardation observed in YC-1-treated tumors.

PDGF is another vasoactive factor that, like VEGF, promotes angiogenesis and growth in solid tumors. PDGF is stored in the α-granules of platelets, and its secretion is stimulated by platelet aggregation *(22)*. Because YC-1 inhibits platelet aggregation, it is possible that some of the antiangiogenic effects of YC-1 are mediated by reduced levels of PDGF in tumors, although such an effect has not before been reported. Thus, to test the possibility that YC-1 inhibits PDGF-induced angiogenesis in tumors, we examined the levels of PDGF-A and PDGF-B protein in Hep3B tumors (Fig. 6, A). No substantial differences in the levels of PDGF-A or PDGF-B were observed in tumors from vehicle- and YC-1-treated mice. This result suggests that the anti-platelet aggregation effect of YC-1 does not appear to affect tumor growth.

Effect of YC-1 on NK Cell Function

The athymic nude mouse, which has no thymus-dependent immunologic functions, is a useful model for assaying tumor growth potential *in vivo*. However, this mouse model has been shown to have thymus-independent NK cells, which are lym-

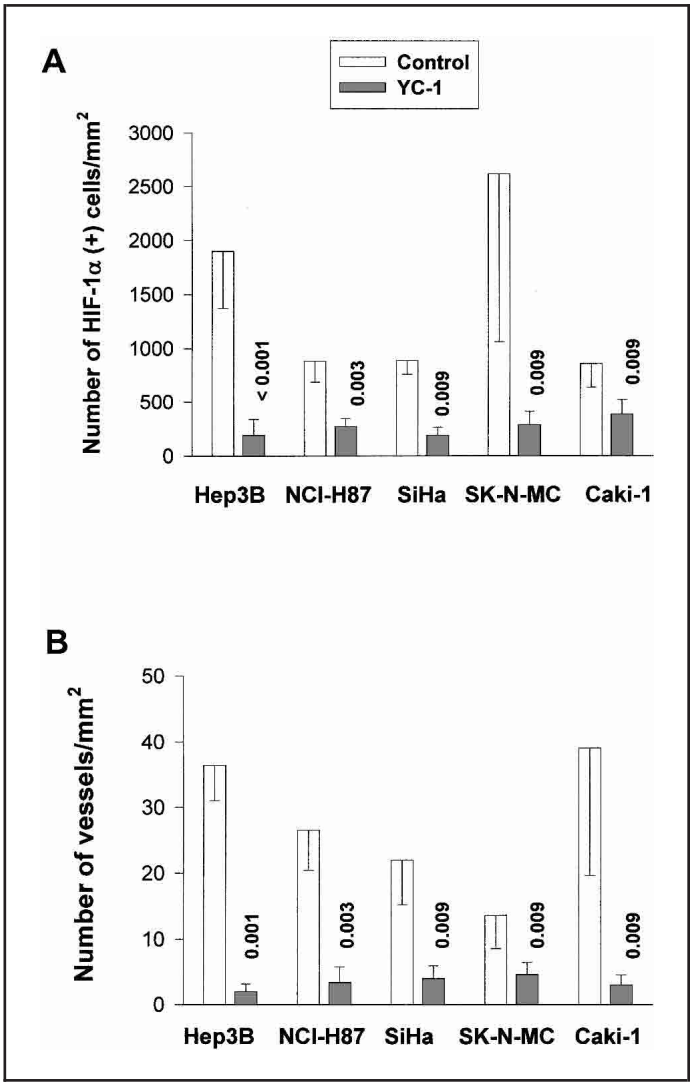

Fig. 5. Quantification of hypoxia-inducible factor 1 alpha (HIF-1α) expression and vascular density detected by immunohistochemistry in human cancer xenografts derived from Hep3B hepatoma, NCI-H87 gastric carcinoma, SiHa cervical carcinoma, SK-N-MC neuroblastoma, or Caki-1 renal carcinoma cells. Viable tumor cells (5×10^6) were injected subcutaneously into the flanks of male nude mice. After the tumors reached 100–150 mm^3 in size, mice received an intraperitoneal injection of YC-1 (30 μg/g) or vehicle (dimethyl sulfoxide [DMSO]) daily for 2 weeks. After the last treatment, the mice were euthanized and the tumors were removed, fixed with formalin, embedded in paraffin, and processed for immunohistochemistry to detect HIF-1α-positive cells (**A**) and CD31-positive vessels (**B**). Two sections per xenograft (5–10 fields per section) were examined for histologic assessment (number of control-treated and YC-1-treated xenografts: n = 24 and 12, respectively, for Hep3B; n = 14 and 12, respectively, for NCI-H87; n = 10 and 10, respectively, for SiHa; n = 10 and 10, respectively, for SK-N-MC; n = 12 and 10, respectively, for Caki-1). Each **bar** represents the mean with lower or upper 95% confidence interval. Statistical significance of differences between treatment groups were compared using a Mann–Whitney *U* test. **Numbers over the error bars** represent the *P* value of the difference relative to the control.

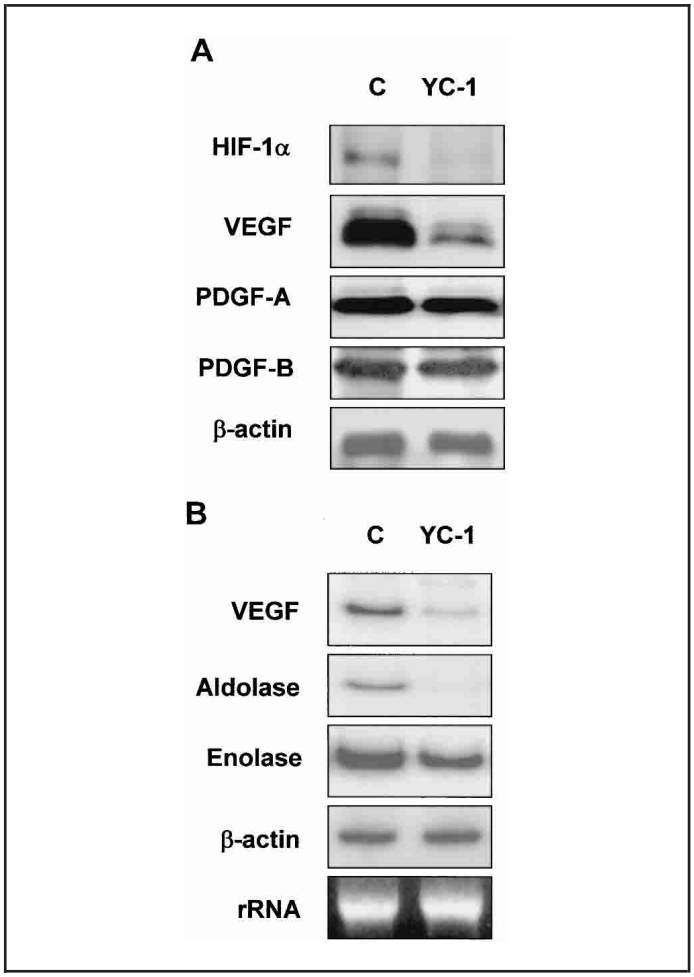

Fig. 6. The effects of YC-1 on the expression of hypoxia-inducible factor 1 alpha (HIF-1α) and hypoxia-inducible genes in Hep3B hepatoma cell xenografts. Viable Hep3B cells (5×10^6) were injected subcutaneously into the flanks of male nude mice. After the tumors reached 100–150 mm^3 in size, mice received an intraperitoneal injection of YC-1 (30 μg/g) or vehicle (dimethyl sulfoxide [DMSO]) daily for 2 weeks. After the last treatment, the mice were euthanized, the tumors removed, and lysates prepared for immunoblotting (**A**) and mRNA analysis by semiquantitative reverse transcription–polymerase chain reaction (RT–PCR). **A**) Tumor lysates from vehicle-treated mice (C) and from YC-1-treated (YC-1) mice were assessed for HIF-1α, vascular endothelial growth factor (VEGF), platelet-derived growth factor (PDGF)-A and PDGF-B, and β-actin protein levels by immunoblotting. **B**) The mRNA levels of VEGF, aldolase A, enolase 1, and β-actin in tumor lysates were measured by semiquantitative RT–PCR *(18).* The quality of the extracted RNAs was verified by identifying the 18S ribosomal RNA (rRNA) on a 1% denaturing agarose gel.

phoid cells with cytolytic activity capable of lysing tumors in the absence of previous stimulation *(23).* Thus, to rule out the possibility that YC-1 inhibits tumor growth by activating NK cells, we examined whether YC-1 affected the cytolytic activity of NK cells *in vitro* and *in vivo.* Splenic lymphocytes incubated with YC-1 *in vitro* had cytolytic activity against NK-cell sensitive YAC-1 cells that was comparable with that from splenic lymphocytes incubated without YC-1 (Fig. 7, A). Moreover, splenic lymphocytes from mice treated with YC-1 for 2 weeks had cytolytic activity that was comparable with that from vehicle-treated mice (Fig. 7, B).

To examine whether there were differences in the number of NK cells that infiltrated the tumors *in vivo,* we quantified the number of NK cells in tumor sections by immunostaining with anti-asialo GM1 antibody (supplemental Fig. 1, available at http://jncicancerspectrum.oupjournals.org/jnci/content/vol95/issue7/index.shtml). NK cells were observed in Hep3B tumor sections from vehicle- and YC-1-treated mice, although the difference in number was not statistically significant (vehicle-treated tumors [n = 6], mean = 8.8 per mm^2, 95% CI = 6.9 to 10.7 per mm^2; YC-1-treated tumors [n = 6], mean = 8.4 per

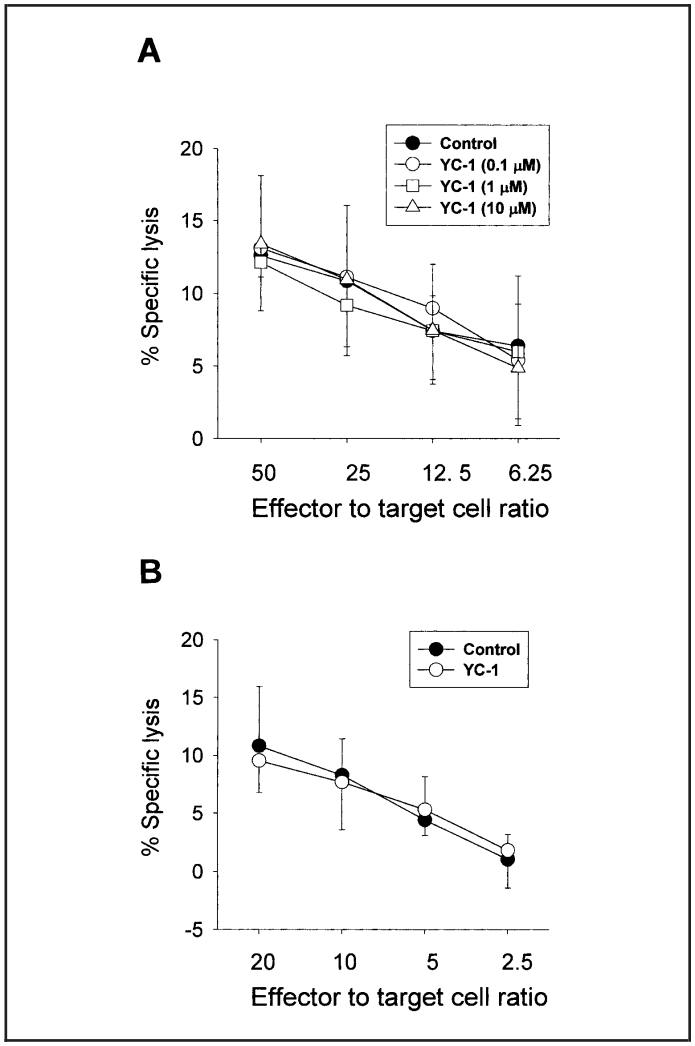

Fig. 7. The effect of YC-1 on natural killer (NK) cell activity. **A**) Splenic lymphocytes (6.25×10^4 to 5×10^5), isolated from male nude mice, were incubated with YC-1 at various concentrations for 24 hours. The lymphocytes were then incubated at the indicated effector : target cell ratios with ^{51}Cr-labeled YAC-1 cells (1×10^4) as described *(21).* After 4 hours, the amount of radioactivity in the culture supernatants was measured with a gamma counter. **B**) Male nude mice (n = 4 per group) received a daily intraperitoneal injection of vehicle (dimethyl sulfoxide [DMSO]) or YC-1 (30 μg/g) for 2 weeks. Splenic lymphocytes were then isolated and tested for NK cell activity. Cytolytic activity was measured three times per experiment. The result is expressed as the mean of four separate experiments with 95% confidence intervals.

mm^2, 95% CI = 5.8 to 11.0 per mm^2, $P = .7$). These results suggest that YC-1 has no effect on NK cell function.

Discussion

Angiogenesis is essential for the growth and metastasis of solid tumors, and the inhibition of angiogenesis is emerging as a promising strategy for cancer treatment *(24).* Because of their role in angiogenesis, VEGF and its receptors have become major targets for antiangiogenic therapy. Indeed, antibodies and soluble proteins that interact with VEGF and its receptors have been investigated as an antiangiogenic therapy for solid tumors *(25).* Angiogenesis is often stimulated by hypoxic conditions such as those that can occur during tumor growth. HIF-1 is a hypoxia-activated transcription factor that can regulate VEGF synthesis. HIF-1 activity is dependent upon the level of available HIF-1α, making this component another good antiangiogenic target *(26).* However, to date, no antitumor agent targeting HIF-1 has been reported. Here, we show that YC-1 has the potential to become the first antiangiogenic anticancer agent to target HIF-1α.

In addition to angiogenesis, changes in energy metabolism are another important adaptation process for cell survival under hypoxia. In hypoxic conditions, oxidative phosphorylation is impaired, and several glycolytic enzymes must be induced to maintain the basal level of adenosine 5′-triphosphate required for cell survival *(27).* Therefore, the inhibitory action of YC-1 on the expression of the aldolase and enolase genes in tumors probably inhibits cell survival under hypoxia and may promote cell death in hypoxic areas. However, no differences were found in the percentage of necrosis in vehicle- and YC-1-treated tumors, suggesting that the decreased expression of the glycolytic enzymes may not contribute substantially to tumor growth inhibition. We conclude that YC-1 appears to halt tumor growth by blocking angiogenesis and not by a direct cytotoxic effect on tumor cells.

YC-1 was developed as an activator of soluble guanylyl cyclase *(28).* It increases the catalytic rate of the enzyme and sensitizes enzyme activation by nitric oxide or carbon monoxide *(29). In vivo,* YC-1 treatment inhibited platelet-rich thrombosis *(15)* and decreased mean arterial pressure *(30),* which were associated with increased cGMP levels in platelet and vascular smooth muscle cells. Thus, we anticipate that, at the dosage used for cancer chemotherapy (30 μg/g), YC-1 would result in increased bleeding time and hypotension. To develop YC-1 as a new anticancer agent, these untoward effects should be carefully evaluated. In our opinion, because these effects are clinically manageable, these potential disadvantages should not restrict the clinical use of YC-1 as an anticancer therapy. Moreover, YC-1 has merit as a cancer chemotherapy agent because of its low cytotoxicity. No serious toxicity was observed in any of the nude mice treated with YC-1 over a 2-week period (data not shown). Furthermore, YC-1 did not suppress the cytolytic activity of splenic lymphocytes *in vitro* or *in vivo.* Thus, we believe that YC-1 is worth investigating further for clinical applications in cancer therapy.

In summary, we tested whether YC-1 could target HIF-1 and inhibit tumor angiogenesis *in vivo.* We confirmed the inhibitory effects of YC-1 on the expression of HIF-1α and on the induction of VEGF, aldolase A, and enolase 1 in cancer cells cultured under hypoxic conditions. *In vivo,* treatment with YC-1 halted the growth of xenograft tumors originating from Hep3B, Caki-1, NCI-H87, SiHa, and SK-N-MC cells. Tumors from YC-1-treated mice showed fewer blood vessels and lower expression of HIF-1α protein and of HIF-1-regulated genes than tumors from vehicle-treated mice. These results suggest that YC-1 is an inhibitor of HIF-1 that halts tumor growth by blocking tumor angiogenesis and tumor adaptation to hypoxia.

References

(1) Hockel M, Vaupel P. Tumor hypoxia: definitions and current clinical, biologic, and molecular aspects. J Natl Cancer Inst 2001;93:266–76.

(2) Dachs GU, Tozer GM. Hypoxia modulated gene expression: angiogenesis, metastasis and therapeutic exploitation. Eur J Cancer 2000;36:1649–60.

(3) Brown JM. The hypoxic cell: a target for selective cancer therapy—eighteenth Bruce F. Cain Memorial Award lecture. Cancer Res 1999;59:5863–70.

(4) Forsythe JA, Jiang BH, Iyer NV, Agani F, Leung SW, Koos RD, et al. Activation of vascular endothelial growth factor gene transcription by hypoxia-inducible factor 1. Mol Cell Biol 1996;16:4604–13.
(5) Wang GL, Semenza GL. Purification and characterization of hypoxia-inducible factor 1. J Biol Chem 1995;270:1230–7.
(6) Maxwell PH, Wiesener MS, Chang GW, Clifford SC, Vaux EC, Cockman ME, et al. The tumour suppressor protein VHL targets hypoxia-inducible factors for oxygen-dependent proteolysis. Nature 1999;399:271–5.
(7) Jaakkola P, Mole DR, Tian YM, Wilson MI, Gielbert J, Gaskell SJ, et al. Targeting of HIF-alpha to the von Hippel-Lindau ubiquitylation complex by O2-regulated prolyl hydroxylation. Science 2001;292:468–72.
(8) Ivan M, Kondo K, Yang H, Kim W, Valiando J, Ohh M, et al. HIFalpha targeted for VHL-mediated destruction by proline hydroxylation: implications for O2 sensing. Science 2001;292:464–8.
(9) Masson N, Willam C, Maxwell PH, Pugh CW, Ratcliffe PJ. Independent function of two destruction domains in hypoxia-inducible factor-alpha chains activated by prolyl hydroxylation. EMBO J 2001;20:5197–206.
(10) Huang LE, Gu J, Schau M, Bunn HF. Regulation of hypoxia-inducible factor 1alpha is mediated by an O2-dependent degradation domain via the ubiquitin-proteasome pathway. Proc Natl Acad Sci U S A 1998;95:7987–92.
(11) Semenza GL. HIF-1 and tumor progression: pathophysiology and therapeutics. Trends Mol Med 2002;8:S62–7.
(12) Zhong H, De Marzo AM, Laughner E, Lim M, Hilton DA, Zagzag D, et al. Overexpression of hypoxia-inducible factor 1alpha in common human cancers and their metastases. Cancer Res 1999;59:5830–5.
(13) Birner P, Schindl M, Obermair A, Plank C, Breitenecker G, Oberhuber G. Overexpression of hypoxia-inducible factor 1alpha is a marker for an unfavorable prognosis in early-stage invasive cervical cancer. Cancer Res 2000;60:4693–6.
(14) Maxwell PH, Dachs GU, Gleadle JM, Nicholls LG, Harris AL, Stratford IJ, et al. Hypoxia-inducible factor-1 modulates gene expression in solid tumors and influences both angiogenesis and tumor growth. Proc Natl Acad Sci U S A 1997;94:8104–9.
(15) Teng CM, Wu CC, Ko FN, Lee FY, Kuo SC. YC-1, a nitric oxide-independent activator of soluble guanylate cyclase, inhibits platelet-rich thrombosis in mice. Eur J Pharmacol 1997;320:161–6.
(16) Galle J, Zabel U, Hubner U, Hatzelmann A, Wagner B, Wanner C, et al. Effects of the soluble guanylyl cyclase activator, YC-1, on vascular tone, cyclic GMP levels and phosphodiesterase activity. Br J Pharmacol 1999;127:195–203.
(17) Chun YS, Yeo EJ, Choi E, Teng CM, Bae JM, Kim MS, et al. Inhibitory effect of YC-1 on the hypoxic induction of erythropoietin and vascular endothelial growth factor in Hep3B cells. Biochem Pharmacol 2001;61:947–54.
(18) Chun YS, Choi E, Yeo EJ, Lee JH, Kim MS, Park JW. A new HIF-1 alpha variant induced by zinc ion suppresses HIF-1-mediated hypoxic responses. J Cell Sci 2001;114:4051–61.
(19) Chun YS, Choi E, Kim TY, Kim MS, Park JW. A dominant-negative isoform lacking exons 11 and 12 of the human hypoxia-inducible factor-1alpha gene. Biochem J 2002;362:71–9.
(20) Kim CH, Cho YS, Chun YS, Park JW, Kim MS. Early expression of myocardial HIF-1alpha in response to mechanical stresses: regulation by stretch-activated channels and the phosphatidylinositol 3-kinase signaling pathway. Circ Res 2002;90:E25–33.
(21) Yajima T, Nishimura H, Wajjwalku W, Harada M, Kuwano H, Yoshikai Y. Overexpression of interleukin-15 in vivo enhances antitumor activity against MHC class I-negative and -positive malignant melanoma through augmented NK activity and cytotoxic T-cell response. Int J Cancer 2002;99:573–8.
(22) Heldin CH, Westermark B. Mechanism of action and in vivo role of platelet-derived growth factor. Physiol Rev 1999;79:1283–316.
(23) Klein AS, Plata F, Jackson MJ, Shin S. Cellular tumorigenicity in nude mice. Role of susceptibility to natural killer cells. Exp Cell Biol 1979;47:430–45.
(24) Folkman J. Tumor angiogenesis: therapeutic implications. N Engl J Med 1971;285:1182–6.
(25) Griffioen AW, Barendsz-Janson AF, Mayo KH, Hillen HF. Angiogenesis, a target for tumor therapy. J Lab Clin Med 1998;132:363–8.
(26) Blagosklonny MV. Hypoxia-inducible factor: Achilles' heel of antiangiogenic cancer therapy. Int J Oncol 2001;19:257–62.
(27) Semenza GL, Roth PH, Fang HM, Wang GL. Transcriptional regulation of genes encoding glycolytic enzymes by hypoxia-inducible factor 1. J Biol Chem 1994;269:23757–63.
(28) Ko FN, Wu CC, Kuo SC, Lee FY, Teng CM. YC-1, a novel activator of platelet guanylate cyclase. Blood 1994;84:4226–33.
(29) Friebe A, Mullershausen F, Smolenski A, Walter U, Schultz G, Koesling D. YC-1 potentiates nitric oxide- and carbon monoxide-induced cyclic GMP effects in human platelets. Mol Pharmacol 1998;54:962–7.
(30) Rothermund L, Friebe A, Paul M, Koesling D, Kreutz R. Acute blood pressure effects of YC-1-induced activation of soluble guanylyl cyclase in normotensive and hypertensive rats. Br J Pharmacol 2000;130:205–8.

NOTES

E. J. Yeo and Y. S. Chun contributed equally to this work.

Manuscript received September 20, 2002; revised January 16, 2003; accepted January 28, 2003.